ChemPhysChem

Research Article
doi.org/10.1002/cphc.202200227

Chemistry Europe
European Chemical Societies Publishing

www.chemphyschem.org

VIP *Very Important Paper*

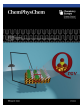

Identification of Electrochemically Adsorbed Species via Electrochemical Microcalorimetry: Sulfate Adsorption on Au(111)

Marco Schönig,[a] Stefan Frittmann,[a] and Rolf Schuster*[a]

We investigate compositional changes of an electrochemical interface upon polarization with electrochemical microcalorimetry. From the heat exchanged at a Au(111) electrode upon sulfate adsorption, we determine the reaction entropy of the adsorption process for both neutral and acidic solutions, where the dominant species in solution changes from SO_4^{2-} to HSO_4^-. In neutral solution, the reaction entropy is about 40 $J\,mol^{-1}\,K^{-1}$ more positive than that in acidic solution over the complete sulfate adsorption region. This entropy offset is explicable by a deprotonation step of HSO_4^- preceding sulfate adsorption in acidic solution, which shows that the adsorbing species is SO_4* in both solutions. The observed overall variation of the reaction entropy in the sulfate adsorption region of ca. 80 $J\,mol^{-1}\,K^{-1}$ indicates significant sulfate-coverage dependent entropic contributions to the Free Enthalpy of the surface system.

Composition and structure of the electrochemical interface are decisive for its activity towards electrochemical processes, ranging from simple electrosorption to catalysis.[1] However, detailed information about the nature and potential-dependent surface coverages of the species at the interface is rather scarce and often limited to the Hg/solution interface, where the measurement of surface tension allows the application of the Gibbs adsorption isotherm.[2] One of the few exceptions is the Au(111) surface in sulfate containing electrolytes. At potentials positive of the potential of zero charge (pzc; ca. 0.55 V vs. reversible hydrogen electrode (RHE) for 1 mM K_2SO_4 in perchlorate supporting electrolyte[3]) sulfate adsorption starts. The surface excess concentration of the sulfate species as a function of the potential was determined in a seminal chronocoulometric study from Lipkowski's group.[3] They found that the sulfate coverage steadily increases up to about 1.15 V vs. RHE and derived from the Essin-Markov coefficient that predominantly SO_4^{2-}(aq) is entering the electrode-solution interface from the solution side, both for adsorption from neutral and acidic solutions, although the prevalent sulfate species in solution changes from SO_4^{2-}(aq) to HSO_4^-(aq). The adsorption of SO_4* (the asterisk (*) indicates the adsorbed sulfate species including its counter charge at the electrode) is further corroborated by several spectroscopic studies, e.g., by surface enhanced infrared absorption spectroscopy (SEIRAS), which found only SO_4* specific bands.[4–6] At ca. 0.9 V vs. RHE an ordered $\left(\sqrt{3}x\sqrt{7}\right)$ structure was observed in several scanning tunneling microscopy (STM) studies in acidic media.[7] From STM images[6,7] and previous density functional theory (DFT) calculations[8] adsorption of HSO_4* or the stabilization of a sulfate structure by coadsorbed H_3O^+ was postulated, which implies that the net adsorbing species, i.e., the species entering the interface is HSO_4^-. However, a recent combined STM, Infrared (IR), Raman, and DFT study by Fang et al.[9] provides strong arguments that the $\left(\sqrt{3}x\sqrt{7}\right)$ structure is comprised of SO_4*, stabilized by a network of coadsorbed water molecules, in accordance with the above mentioned chronocoulometric study. Although the discussion of the ordered sulfate structure has converged, there is still an ongoing debate about the nature of the sulfate species at intermediate coverages, i.e., at potentials below that of the $\left(\sqrt{3}x\sqrt{7}\right)$ structure formation. By DFT calculations Fang et al.[9] assigned a band, found in experimental Raman spectra at lower potentials, to a H_2O…HSO_4 stretching mode and excluded several adlayer configurations containing SO_4* based on their theoretically expected spectral signatures. In addition, DFT calculations on the stability of ordered sulfate adlayers showed that at lower potentials a HSO_4*-water structure should become stable. This is in accordance with a DFT study by Gossenberger et al.,[10] where a sequence of ordered mixed HSO_4*/SO_4* structures was found. In these structures the SO_4* content increases with higher potentials, ultimately leading to a $\left(\sqrt{3}x\sqrt{7}\right)$ SO_4* adlayer. These results contrast the results from Lipkowski's group, which found that SO_4* is the predominantly adsorbed species in the whole sulfate adsorption region. However, as stated in Ref. [8], disordered structures are naturally not considered by the slab models used for DFT calculations and other possible processes such as structural transformations of disordered SO_4* phases cannot be ruled out.

In the current paper we present thermodynamic data on the reaction entropy of the sulfate adsorption process on Au(111) in neutral and acidic sulfate-containing solutions. Thus,

[a] *M. Schönig, Dr. S. Frittmann, Prof. Dr. R. Schuster*
Institute of Physical Chemistry,
Karlsruhe Institute of Technology
Kaiserstraße 12, 76131 Karlsruhe, Germany
E-mail: rolf.schuster@kit.edu

Supporting information for this article is available on the WWW under https://doi.org/10.1002/cphc.202200227

if the adsorbed species were SO_4*, the adsorption step in acidic solution would have to be preceded by deprotonation of HSO_4^-(aq), whereas in neutral solution SO_4^{2-}(aq) could be directly adsorbed. Vice versa, for HSO_4* adsorption, in neutral solution a protonation step of SO_4^{2-}(aq) had to precede HSO_4* adsorption. Therefore, by measuring the difference of the reaction entropies for sulfate adsorption from acidic and neutral solution we can identify the nature of the preceding reaction step and thus the adsorbing species.

To determine the reaction entropy of the adsorption process, we measure the heat generated at a Au(111) electrode upon minute polarization, whereby the sulfate coverage changes by less than 1% of a monolayer. In an electrochemical cell the heat reversibly exchanged with the surrounding, that is, close to equilibrium conditions, corresponds to the reaction entropy of the cell reaction multiplied by the temperature *T*. While this holds true for full cells, when considering single electrodes, charge transport across the borders of the half-cell has to be taken into account. Then, close to thermal equilibrium the heat corresponds to the reaction entropy of the half-cell reaction $\Delta_R S$ plus a contribution from transport $\Delta_T S$, which is determined by ion transport in solution and electron transport in the metal electrode. The exchanged molar heat of a reversible half-cell reaction, called molar Peltier heat Π, is given by $\Pi = -T(\Delta_R S + \Delta_T S)$. In the current paper, $(\Delta_R S + \Delta_T S)$ gives the entropy change during the (anodic) sulfate adsorption process. A positive Peltier heat thus signals a negative entropy change at the interface. A detailed description of the theoretical background can be found e.g. in Ref. [11]. Details of the experimental setup and the underlying principles of our microcalorimeter can be found in Refs. [12,13]. In brief, the exchanged heat is determined from the temperature change at the electrode, measured by a 25 μm pyroelectric $LiTaO_3$ sensor at the back of a thin electrode, consisting of a 200 nm Au film on a 50 μm sapphire sheet (active area 0.2 cm^2). The electrochemical processes are driven by 10 ms potential or current pulses, which is fast enough to avoid substantial heat loss into the electrolyte, but slow enough to follow the temperature change at the electrode's backside. Calibration of the calorimeter was performed by comparison with the heat exchange during the electron transfer reaction in $[Fe(CN)_6]^{3+/4+}$, for which the Peltier heat is known from literature, under consideration of the thermal response function of the electrochemical cell (see Ref. [12] and Supporting Information). The Au film was prepared by flame annealing in a butane-gas flame, yielding a predominately (111)-textured surface. Electrolyte solutions were prepared from H_2SO_4 (suprapure, Merck), K_2SO_4 (suprapure, Merck) and ultrapure water (18.2 Ω cm, Arium, Sartorius). The solutions were deaerated by argon bubbling and subsequently transferred to a closed EC cell under argon atmosphere. Pt wires were employed as pseudo-reference and counter electrodes.

Figure 1 shows a typical cyclic voltammogram (CV) of a (111)-textured Au film in 0.1 M H_2SO_4 (black line, left axis). The potential is referenced versus RHE in accordance with Ref. [5]. Relative to this reference electrode the potential for sulfate adsorption becomes independent of the solution pH.[5] With lower sulfate concentration, the potential of the sulfate adsorption region shifts slightly positive, by about 0.05 V upon dilution by a factor of 10.[14] The CV exhibits all relevant features reported in the literature for this system (see Refs. [3,15] for a detailed discussion). The anodic current peak at E = 0.55 V originates from the lifting of the gold reconstruction, which is induced by the beginning sulfate adsorption.[16] With increasing potential the sulfate coverage constantly increases, until at ca. E = 1.09 V a $\left(\sqrt{3}x\sqrt{7}\right)$ R19° anion adlayer forms, indicated by a small reversible peak pair in the CV. Albeit on very well ordered (111) surfaces with large terraces those peaks may become very narrow and eventually excel the other peaks, their presence already indicates a rather well defined (111) texture with terrace sizes of at least 20 atoms.[5]

Figure 1a also includes the molar heat of the sulfate adsorption process (right axis, red and blue triangles, green

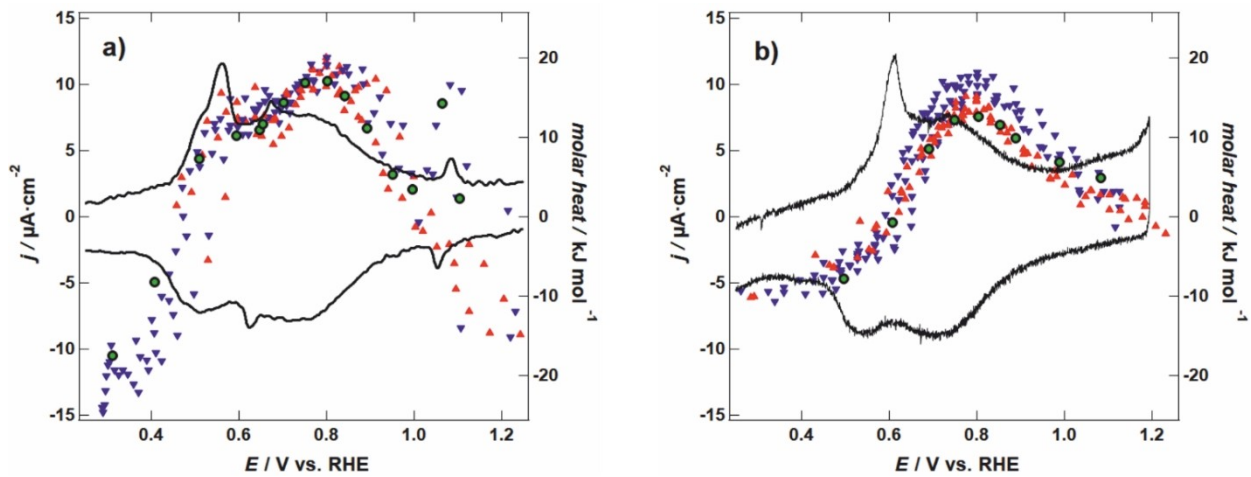

Figure 1. a) Cyclic voltammogram (left axis, black line) and molar heat (right axis) of sulfate adsorption on Au(111) in 0.1 M H_2SO_4. The red, upward or blue, downward triangles represent molar heat values obtained by series of positive or negative current pulses of 50 and 100 μA amplitude and 10 ms duration. The green circles mark the Peltier heat obtained from 10 ms potential pulses of varying amplitude and polarity, starting at the respective potential. For further explanation, see text. b) same as in a) for Au(111) in 0.1 M K_2SO_4.

circles), which is the heat referenced to the charge equivalents that flowed in the outer cell circuit during the electrode polarization. The data originates from three slightly different experimental procedures, described in detail in the supporting information and in ref.:[17] i) The red upward triangles mark the molar heat values upon charging the electrode by a series of 10 ms, 50 or 100 μA positive current pulses. These pulse series started at a potential of about 0.4 V. Due to the positive current pulses, the potential raised positively by typically a few mV per current pulse. ii) Similar to i), now charging with 10 ms negative, −50 or −100 μA current pulses (blue downward triangles). These pulse series started at about 1.2 V. iii) Potentiostatic pulse series (green circles), where 10 ms long, alternating positive and negative potential pulses with varying amplitudes were applied starting at a fixed base potential. The molar Peltier heat is obtained by extrapolation of the molar heat values towards zero pulse amplitude. Example potential-, current- and temperature-transients are presented in the supporting information. The molar heat values of all three experimental procedures coincide. Note that a positive molar heat corresponds to warming upon positive current or potential pulses and cooling during negative pulses. The coincidence of the data for different pulse polarities of series i) and ii) signals a high degree of reversibility of the sulfate adsorption process. Thus, the molar heat obtained by the current pulse experiments corresponds essentially to the molar Peltier heat of the electrode reaction.

In Figure 1b we show equivalent data for sulfate adsorption on Au(111) in 0.1 M K_2SO_4. Despite the predominant ion in solution is now SO_4^{2-}(aq), the CV strongly resembles that of the acidic solution in Figure 1a, concerning its overall shape as well as the flowed charge. This is in accordance with literature, e.g., ref.[3] and already signals the similarity of the sulfate adsorption process in both solutions. The variation of the molar heat with potential also coincides with that in Figure 1a, with the values of the molar heat being slightly lower by a few kJ mol^{-1}.

From the Peltier heat, the reaction entropy for the adsorption process can be extracted by consideration of the entropy contribution from transport $\Delta_T S$ (details are given in the supporting information). The resulting molar reaction entropy for the sulfate adsorption process $\Delta_R S$ on Au(111) in 0.1 M H_2SO_4 and 0.1 M K_2SO_4, obtained as average of pulse series from five experiments, is shown by orange circles (acidic solution) and violet squares (neutral solution) in Figure 2a. The error bars give the standard deviation of the reaction entropy at different potentials. They also include errors due to irreversible heat contributions in the molar heat data obtained by current pulses. The averaged entropy data nicely follow the variation of the molar heat with potential of Figure 1 (with inversed sign). Due to the averaging, the pronounced peaks found for the molar heat in individual experiments are slightly smeared out. The curves for acidic and neutral solution run strikingly parallel to each other, with the reaction entropy in the neutral solution being higher by about 45 J mol^{-1} K^{-1} at all potentials. Equivalent results were found in 0.01 M solutions of H_2SO_4 and K_2SO_4 (Figure 2b), were the entropy difference between neutral and acidic solutions is slightly smaller (ca. 30 J mol^{-1} K^{-1}).

The overall variation of the reaction entropy in the sulfate adsorption region for a single electrolyte in Figure 2 amounts to about 80 J mol^{-1} K^{-1} between the minimum at intermediate sulfate coverages and the maximum values around 0.4 and 1.2 V. This implies a variation of the entropic contribution to the Free Enthalpy of the surface system of 300 K·80 J mol^{-1} K^{-1} = 24 kJ mol^{-1}, which corresponds to 0.23 V on the potential scale and points to the importance of entropic contributions for the stability of the surface phase. The variation of the entropy may be attributed to changes of the configurational entropy of the sulfate adlayer with coverage, similar to observations made for

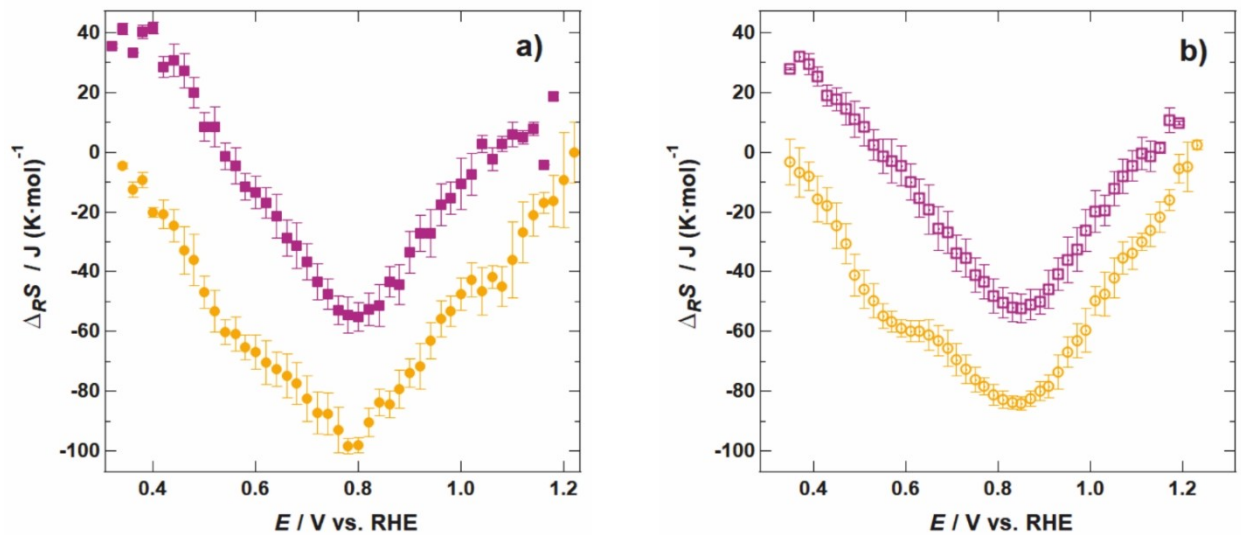

Figure 2. a) Potential dependent molar entropy for sulfate adsorption on Au(111) in 0.1 M H_2SO_4 (orange open circles) and 0.1 M K_2SO_4 (violet open squares). The data represents the average of pulse series from five experiments. b) Molar entropy for Au(111) in 0.01 M H_2SO_4 (orange circles) and 0.01 M K_2SO_4 (violet squares), obtained by averaging of pulse series from three experiments.

DL charging in ionic liquids.[18] Note that the strong increase of the reaction entropy at higher potentials/sulfate coverages cannot be explained by a simple lattice gas model but signals the involvement of interactions between the adsorbed sulfate species.[19] Also contributions from ordering of water in the high field of the double layer should be considered (see discussions, e.g., in Refs. [4, 20]). A more detailed explanation of these entropy variations seems impossible based on the current data and is beyond the scope of the current paper. However, this does not impede to draw conclusions on the adsorption process and the adsorbing species, as shown in the following.

Figure 2 shows that the reaction entropy of the sulfate adsorption process exhibits nearly identical variations in acidic and neutral solutions over the whole sulfate adsorption region. This strongly implies that the constitution and structure of the interface layer is the same in both solutions. This finding is in agreement, e.g., with the chronocoulometric study of Lipkowski's group[3,21] and with radioactive labeling experiments by Zelenay et al, who showed that the adsorbing species is the same in neutral and acidic solutions.[22] Also SEIRAS by Ataka et al. and Wandlowski et al. pointed out that the spectroscopic features stay the same in neutral and acidic solutions for sulfate adsorption on Au(111).[4,5]

Thus, it is reasonable to conclude that the adsorbing species is identical in neutral and acidic solutions and that the offset of the respective entropy curves in Figure 2a or b is determined by the reaction entropy of a preceding reaction step, which would be deprotonation of HSO_4^-(aq) for SO_4* adsorption or protonation of SO_4^{2-}(aq) for adsorption of HSO_4*. Since protonation or deprotonation occur in solution, the corresponding reaction entropy can be readily calculated from the molar entropies of the species in solution, considering the detailed speciation of the electrolyte solutions. Table 1 summarizes the results for the calculated difference, $\Delta\Delta_R S$, between the reaction entropies in neutral and acidic solutions for 0.1 M and 0.01 M sulfate concentration, considering the specific speciation of the electrolytes (for details on the speciation and the calculation see supporting information). The experimental values determined from the data in Figure 2 are also included in Table 1, with errors representing the standard deviation of the averaged data.

In Table 1 the experimentally determined entropy differences match the values calculated for pure SO_4* adsorption within their error bars, clearly showing that only SO_4* adsorption is compatible with the experimental finding at all sulfate coverages, i.e., potentials. There is no indication of considerable coadsorption of SO_4* and HSO_4*, whereupon the theoretical $\Delta\Delta_R S$ would linearly vary between the values for the pure adsorption phases, dependent on the ratio of adsorbed SO_4* and HSO_4*. Thus our results strongly corroborate the original proposition of predominant SO_4* adsorption by Lipkowski's group.[3] It should be noted here that Zhang et al. recently solved a similar discrepancy for sulfate adsorption on Pt(111). By studying the changes of vibrational sum frequency spectra of the sulfate adlayer upon isotope exchange,[23] they came to the conclusion that SO_4* is the adsorbing species also for Pt(111) in sulfate solutions.

Table 1. Difference between the reaction entropies in neutral and acidic solutions $\Delta\Delta_R S$, calculated for SO_4* and HSO_4* adsorption; experimental values from Figure 2.

	SO_4*	HSO_4*	Exp.
$\Delta\Delta_R S$ ($J\,mol^{-1}K^{-1}$); 0.1 M	39	−40	45 ± 9
$\Delta\Delta_R S$ ($Jmol^{-1}K^{-1}$); 0.01 M	23	−54	30 ± 9

In conclusion, we showed that measurements of the reaction entropy of adsorption processes provide information on the net adsorption process and the composition of the interface, which complements the charge-potential relationship, measured usually, e.g., by cyclic voltammetry or coulometry. As a side result, our measurements demonstrate the importance of entropic contributions to the Free Enthalpy of the surface system of adsorbed layers, which in the present case vary by more than 0.23 eV over the sulfate adsorption potential region.

Acknowledgements

We acknowledge funding by the Deutsche Forschungsgemeinschaft (SCHU 958/7-2). Contributions of Vadym Halka during the first stages of the experiments are gratefully acknowledged. Open Access funding enabled and organized by Projekt DEAL.

Conflict of Interest

The authors declare no conflict of interest.

Data Availability Statement

The data that support the findings of this study are available from the corresponding author upon reasonable request.

Keywords: calorimetry · entropy · electrochemistry · electrochemical interfaces · adsorption

[1] a) P. Rodriguez, M. T. M. Koper, *Phys. Chem. Chem. Phys.* **2014**, *16*, 13583–13594; b) D. V. Tripkovic, D. Strmcnik, D. van der Vliet, V. Stamenkovic, N. M. Markovic, *Faraday Discuss.* **2009**, *140*, 25–40; c) S. Hong, S. Lee, S. Kim, J. K. Lee, J. Lee, *Catal. Today* **2017**, *295*, 82–88.
[2] a) D. C. Grahame, *Chem. Rev.* **1947**, *41*, 441–501; b) J. A. Harrison, J. E. B. Randles, D. J. Schiffrin, *J. Electroanal. Chem.* **1973**, *48*, 359–381.
[3] Z. Shi, J. Lipkowski, M. Gamboa, P. Zelenay, A. Wieckowski, *J. Electroanal. Chem.* **1994**, *366*, 317–326.
[4] K. Ataka, M. Osawa, *Langmuir* **1998**, *14*, 951–959.
[5] T. Wandlowski, K. Ataka, S. Pronkin, D. Diesing, *Electrochim. Acta* **2004**, *49*, 1233–1247.
[6] G. J. Edens, *J. Electroanal. Chem.* **1994**, 357–366.
[7] O. M. Magnussen, J. Hageböck, J. Hotlos, R. J. Behm, *Faraday Discuss.* **1992**, *94*, 329–338.
[8] F. C. Simeone, D. M. Kolb, S. Venkatachalam, T. Jacob, *Angew. Chem.* **2007**, *119*, 9061–9064; *Angew. Chem. Int. Ed.* **2007**, *46*, 8903–8906.
[9] Y. Fang, S.-Y. Ding, M. Zhang, S. N. Steinmann, R. Hu, B.-W. Mao, J. M. Feliu, Z.-Q. Tian, *J. Am. Chem. Soc.* **2020**, *142*, 9439–9446.
[10] F. Gossenberger, F. Juarez, A. Groß, *Front. Chem.* **2020**, *8*, 634.

[11] a) J. N. Agar, *Adv. Electrochem. Electrochem. Eng.*; b) E. D. Eastman, *J. Am. Chem. Soc.* **1926**, *48*, 1482–1493; c) R. Schuster, *Curr. Opin. Electrochem.* **2017**, *1*, 88–94; d) T. Ozeki, N. Ogawa, K. Aikawa, I. Watanabe, S. Ikeda, *J. Electroanal. Chem.* **1983**, *145*, 53–65.
[12] K. R. Bickel, K. D. Etzel, V. Halka, R. Schuster, *Electrochim. Acta* **2013**, *112*, 801–812.
[13] S. Frittmann, V. Halka, C. Jaramillo, R. Schuster, *Rev. Sci. Instrum.* **2015**, *86*, 64102.
[14] H. Angerstein-Kozlowska, B. E. Conway, A. Hamelin, L. Stoicoviciu, *J. Electroanal. Chem.* **1987**, *228*, 429–453.
[15] A. Cuesta, M. Kleinert, D. M. Kolb, *Phys. Chem. Chem. Phys.* **2000**, *2*, 5684–5690.
[16] a) D. M. Kolb, J. Schneider, *Electrochim. Acta* **1986**, *31*, 929–936; b) J. Wang, B. M. Ocko, A. J. Davenport, H. S. Isaacs, *Phys. Rev. B* **1992**, *46*, 10321–10338.
[17] S. Frittmann, V. Halka, R. Schuster, *Angew. Chem. Int. Ed.* **2016**, *55*, 4688–4691; *Angew. Chem.* **2016**, *128*, 4766–4769.
[18] J. Lindner, F. Weick, F. Endres, R. Schuster, *J. Phys. Chem. C* **2020**, *124*, 693–700.
[19] a) M. T. M. Koper, *J. Electroanal. Chem.* **1998**, *450*, 189–201; b) J. H. K. Pfisterer, U. E. Zhumaev, W. Cheuquepan, J. M. Feliu, K. F. Domke, *J. Chem. Phys.* **2019**, *150*, 41709.
[20] a) J. Bockris, *J. Electroanal. Chem.* **1975**, *65*, 473–489; b) R. Guidelli, G. Aloisi, E. Leiva, W. Schmickler, *J. Phys. Chem.* **1988**, *92*, 6671–6675.
[21] Z. Shi, J. Lipkowski, S. Mirwald, B. Pettinger, *J. Electroanal. Chem.* **1995**, *396*, 115–124.
[22] P. Zelenay, L. M. Rice-Jackson, A. Wieckowski, *J. Electroanal. Chem.* **1990**, *283*, 389–401.
[23] I. Y. Zhang, G. Zwaschka, Z. Wang, M. Wolf, R. K. Campen, Y. Tong, *Phys. Chem. Chem. Phys.* **2019**, *21*, 19147–19152.

Manuscript received: April 5, 2022
Revised manuscript received: April 28, 2022
Accepted manuscript online: May 5, 2022
Version of record online: July 5, 2022